

**Variations in Stratospheric Inorganic Chlorine
Between 1991 and 2006**

D.J. Lary^{1,2}, D.W. Waugh³, A.R. Douglass², R.S. Stolarski², P.A. Newman²,
H. Mussa⁴

D.J. Lary, Goddard Earth Sciences and Technology Centre, University of Maryland Baltimore
County, Baltimore, MD 21228 (David.Lary@umbc.edu)

¹Goddard Earth Sciences and Technology
Centre, University of Maryland Baltimore
County, Baltimore, Maryland, USA

²Atmospheric Chemistry and Dynamics
Branch, NASA, Goddard Space Flight
Centre, Greenbelt, Maryland, USA

³The Department of Earth & Planetary
Sciences Maryland, Johns Hopkins
University, Baltimore, USA

⁴Department of Chemistry, University of
Cambridge, England

3 A consistent time series of stratospheric inorganic chlorine Cl_y from 1991
4 to present is formed using space-borne observations together with neural net-
5 works. A neural network is first used to account for inter-instrument biases
6 in HCl observations. A second neural network is used to learn the abundance
7 of Cl_y as a function of HCl and CH_4 , and to form a time series using avail-
8 able HCl and CH_4 measurements. The estimates of Cl_y are broadly consis-
9 tent with calculations based on tracer fractional releases and previous esti-
10 mates of stratospheric age of air. These new estimates of Cl_y provide a crit-
11 ical test for current global models that predict significant differences in Cl_y
12 and ozone recovery.

1. Introduction

Knowledge of the distribution of inorganic chlorine Cl_y in the stratosphere is needed to attribute changes in stratospheric ozone to changes in halogens, and to assess the realism of chemistry-climate models [Eyring *et al.*, 2006; Eyring, 2007]. However, there are limited direct observations of Cl_y . Simultaneous measurements of the major inorganic chlorine species are rare [Zander *et al.*, 1992; Gunson *et al.*, 1994; Bonne *et al.*, 2000; Nassar *et al.*, 2006]. In the upper stratosphere, Cl_y can be inferred from HCl alone (e.g., Anderson *et al.* [2000]).

Here we combine observations from several space-borne instruments using neural networks [Lary and Mussa, 2004] to produce a time series for Cl_y . A neural network is used to characterize differences among various HCl measurements, and to perform an inter-instrument bias correction. Measurements from several different instruments are used in this analysis. These instruments, together with temporal coverage and measurement uncertainties, are listed in Table 1. All instruments provide measurements through the depth of the stratosphere. A second neural network is used to infer Cl_y from these corrected HCl measurements and measurements of CH_4 .

Sections 2 and 3 describe the the HCl and Cl_y intercomparisons. Section 4 present a summary.

2. HCl Intercomparison

We first compare measurements of HCl from different instruments listed in Table 1. Comparisons are made in equivalent PV latitude - potential temperature coordinates [Schoeberl *et al.*, 1989; Proffitt *et al.*, 1989; Lait *et al.*, 1990; Douglass *et al.*, 1990; Lary

et al., 1995; *Schoeberl et al.*, 2000] to extend the effective latitudinal coverage of the measurements and identify contemporaneous measurements in similar air masses.

The Halogen Occultation Experiment (HALOE) provides the longest record of space based HCl observations. Figure 1 compares HALOE HCl with HCl observations from (a) the Atmospheric Trace Molecule Spectroscopy Experiment (ATMOS), (b) the Atmospheric Chemistry Experiment (ACE) and (c) the Microwave Limb Sounder (MLS). In these plots each point is the median HCl observation made by the instrument during each month for 30 equivalent latitude bins from pole to pole and 25 potential temperature bins from the 300-2500 K potential temperature surfaces.

A consistent picture is seen in these plots: HALOE HCl measurements are lower than those from the other instruments. The slopes of the linear fits (relative scaling) are 1.05 for the HALOE-ATMOS comparison, 1.09 for the HALOE-MLS, and 1.18 for the HALOE-ACE. The offsets are apparent at the 525 K isentropic surface and above. Previous comparisons among HCl datasets reveal a similar bias for HALOE [*Russell et al.*, 1996; *McHugh et al.*, 2005; *Froidevaux et al.*, 2006]. ACE and MLS HCl measurements are in much better agreement [Figure 1(d)]. Note, all measurements agree within the stated observational uncertainties summarized in Table 1.

To combine the above HCl measurements to form a continuous time series of HCl (and then Cl_y) from 1991 to 2006 it is necessary to account for the biases between data sets. A neural network is used to learn the mapping from one set of measurements onto another as a function of equivalent latitude and potential temperature [*Lary and Mussa*, 2004]. We consider two cases. In one case ACE HCl is taken as the reference and the HALOE and

Aura HCl observations are adjusted to agree with ACE HCl. In the other case HALOE HCl is taken as the reference and the Aura and ACE HCl observations are adjusted to agree with HALOE HCl. In both cases we use equivalent latitude and potential temperature to produce average profiles. The purpose of the mapping is simply to learn the bias as a function of location, not to imply which instrument is correct.

The precision of the correction using the neural network mapping is of the order of ≈ 0.3 ppbv, as seen in Figure 1(e) which shows the results when HALOE HCl measurements have been mapped into ACE measurements. The mapping has removed the bias between the measurements and has also straightened out the ‘wiggles’ in 1 (c), i.e., the neural network has learned the equivalent PV latitude and potential temperature dependence of the bias between HALOE and MLS. The inter-instrument offsets are not constant in space or time, and are not a simple function of Cl_y .

3. Inorganic Chlorine Cl_y

To a first approximation $\text{Cl}_y \approx \text{HCl} + \text{ClONO}_2 + \text{ClO}$ [Brasseur and Solomon, 1987], and Cl_y can be estimated from HCl and ClONO_2 . However, observations of ClONO_2 are much more limited than from HCl. As shown in Table 1, ClONO_2 measurements have been made by the CLAES (1991-1993), ATMOS (1992-1994), CRISTA (1994, 1998), and ACE (2004-present).

Because of the limited temporal coverage of ClONO_2 measurements it is not possible to form a continuous time series of Cl_y by combining HCl, ClONO_2 , and ClO. However, it is possible to form a time series of Cl_y using a neural network. There are sufficient observations of ClONO_2 from ATMOS, CLAES, CRISTA, and ACE to train a neural

network to learn the Cl_y abundance as a function of HCl and CH_4 , for each of which there is a long, near-continuous, time series of measurements. The resulting reconstruction reproduces an independent validation dataset faithfully with a correlation coefficient of 0.99, and provides a scatter diagram with a slope very close to one for the observed Cl_y plotted against the neural network inferred Cl_y , see Figure 1(f).

The inputs to the neural network that estimates Cl_y are HCl, CH_4 , equivalent latitude and potential temperature. HCl is used because it is continuously observed from the launch of UARS to the present and is typically the major Cl_y reservoir. CH_4 is used because it is continuously observed from the launch of UARS to the present and, as a long-lived tracer, it is well correlated with Cl_y . Potential temperature and equivalent latitude are used because the correlation between long-lived tracers such as CH_4 and Cl_y is a strong function of altitude and a weak function of latitude [Lary and Mussa, 2004].

Other training strategies using more species were examined. For example, we tested the effectiveness of a neural network with inputs of HCl, O_3 , CH_4 , H_2O , equivalent latitude and potential temperature to estimate Cl_y . This was tried as O_3 , CH_4 and H_2O are key observed species involved in the partitioning of reactive chlorine. When chlorine atoms are released from the chlorine containing source gases by photolysis, they react with CH_4 to form HCl. Alternatively, Cl atoms may react with ozone to form ClO, and then ClO will combine with NO_2 to form ClONO₂. HCl is destroyed either by reaction with OH, photolysis or heterogeneous reactions. The amount of OH present depends on the photolysis of ozone to form $\text{O}(^1\text{D})$ and the subsequent reaction of $\text{O}(^1\text{D})$ with H_2O .

This approach also gave good results, but with slightly lower skill than just using HCl, CH₄, equivalent latitude and potential temperature to estimate Cl_y.

Figure 2 shows how Cl_y profiles estimated by the neural network agree with observed Cl_y for October 2006. In each case the shaded range represents the uncertainty associated with the Cl_y estimate. We note that the HCl bias between HALOE and ACE is the major uncertainty.

The distribution of Cl_y is expected to change between 1991 and 2006 as the abundances of its source gases have changed. Figure 3 shows the time-series of Cl_y for the 525 K isentropic surface (\approx 20 km) and the 800 K isentropic surface (\approx 30 km), for three different equivalent latitudes. The upper limit of each shaded range corresponds to the estimate of Cl_y for the neural network calibrated to agree with ACE v2.2 HCl, and the lower limit to the estimate of Cl_y for the neural network calibrated to agree with HALOE v19 HCl.

The variation in Cl_y estimates between the two cases depends on latitude, altitude and season and is typically ≤ 0.4 ppbv at 800 K. This uncertainty is primarily due to the discrepancy between the different observations of HCl which translates into the Cl_y uncertainty shown by the shading in Figure 3. There is also a slight low bias in the lower stratosphere due to not including HOCl in the estimates of Cl_y. HOCl was not included because HOCl has been observed by ACE only since the start of 2004. Ignoring HOCl is only of significance in regions of strong chlorine activation at low temperatures in the lower stratosphere where HOCl can comprise up-to about 10% of Cl_y.

There is a general tendency of Cl_y to increase in the 1990s, peak around 2000, and then slowly decrease. This is consistent with our expectations based on the tropospheric abundance of chlorine containing source gases. The Cl_y time-series shown in Figure 3 constitutes a useful test for model simulations. The variation in simulated Cl_y from the chemistry-climate models used in the recent *WMO* [2006] report is much greater than the above uncertainty in Cl_y . For example, the simulated peak Cl_y in October at 80S varies from less than 1 ppbv to over 3.5 ppbv, while the peak annual-mean Cl_y for north mid-latitudes varies from 0.8 to 2.8 ppb [Eyring *et al.*, 2006; Eyring, 2007].

The estimates of Cl_y produced are broadly consistent with calculations based on tracer fractional releases [Newman *et al.*, 2006] and previous estimates of stratospheric age of air. Observations show that at 20 km the mean age increases from around 2 years in the tropics to around 4 years at high latitudes (60°N), with a similar gradient at 30 km but older ages by around 2 years [Vaugh and Hall, 2002]. The curves in Figure 3 show calculations of Cl_y for a range values of the mean age of air, and the ages that are required to match the observed Cl_y are consistent with the observations of the mean age.

4. Summary

A consistent time series of stratospheric Cl_y from 1991 to present has been formed using available space-borne observations. Here we used neural networks to inter-calibrate HCl measurements from different instruments, and to estimate Cl_y from observations of HCl and CH_4 . These estimates of Cl_y peaked in the late 1990s and have begun to decline as expected from tropospheric measurements of source gases and troposphere to stratosphere transport times. Furthermore, the estimates of Cl_y produced are consistent

139 with calculations based on tracer fractional releases and age of air [*Newman et al.*, 2006].
140 The Cl_y time-series formed here is an important benchmark for models being used to
141 simulate the recovery of the ozone hole. Although there is uncertainty in the estimates
142 of Cl_y , primarily due to biases in HCl measurements, this uncertainty is small compared
143 with the range of model predictions shown in the recent *WMO* [2006] report. The two
144 Cl_y time-series are available in the electronic supplement.

145 **Acknowledgments.** It is a pleasure to acknowledge NASA for research funding, Lu-
146 cien Froidevaux and the Aura MLS team for their data, the ACE team, Peter Bernath,
147 Chris Boone, and Kaley Walker for their data, the HALOE team and Ellis Remsberg for
148 their data, and the ATMOS team for their data.

References

- 149 Anderson, J., J. M. Russell, S. Solomon, and L. E. Deaver, Halogen occultation experi-
150 ment confirmation of stratospheric chlorine decreases in accordance with the montreal
151 protocol, *J. Geophys. Res. (Atmos.)*, *105*(D4), 4483–4490, 2000.
- 152 Bernath, P. F., et al., Atmospheric chemistry experiment (ace): Mission overview, *Geo-*
153 *phys. Res. Lett.*, *32*(15), 115S01, 2005.
- 154 Bonne, G. P., et al., An examination of the inorganic chlorine budget in the lower strato-
155 sphere, *J. Geophys. Res. (Atmos.)*, *105*(D2), 1957–1971, 2000.
- 156 Brasseur, G., and S. Solomon, *Aeronomy of the Middle Atmosphere : Chemistry and*
157 *Physics of the Stratosphere and Mesosphere*, Atmospheric Science Library, second ed.,
158 D Reidel Pub Co, 1987.
- 159 Douglass, A., R. Rood, R. Stolarski, M. Schoeberl, M. Proffitt, J. Margitan, M. Loewen-
160 stein, J. Podolske, and S. Strahan, Global 3-dimensional constituent fields derived from
161 profile data, *Geophys. Res. Lett.*, *17*(4 SS), 525–528, 1990.
- 162 Eyring, V., et al., Assessment of temperature, trace species, and ozone in chemistry-
163 climate model simulations of the recent past, *J. Geophys. Res. (Atmos.)*, *111*(D22),
164 2006.
- 165 Eyring, V. e. a., Multi-model projections of stratospheric ozone in the 21st century, *J.*
166 *Geophys. Res. (Atmos.)*, *submitted*, 2007.
- 167 Froidevaux, L., et al., Early validation analyses of atmospheric profiles from EOS MLS
168 on the aura satellite, *IEEE Trans. Geosci. Remote Sens.*, *44*(5), 1106–1121, 2006.

- Gunson, M. R., M. C. Abrams, L. L. Lowes, E. Mahieu, R. Zander, C. P. Rinsland,
M. K. W. Ko, N. D. Sze, and D. K. Weisenstein, Increase in levels of stratospheric
chlorine and fluorine loading between 1985 and 1992, *Geophys. Res. Lett.*, *21*(20), 2223–
2226, 1994.
- Lait, L., et al., Reconstruction of O₃ and N₂O fields from ER-2, DC-8, and balloon obser-
vations, *Geophys. Res. Lett.*, *17*(4 SS), 521–524, 1990.
- Lary, D., M. Chipperfield, J. Pyle, W. Norton, and L. Riishojgaard, 3-dimensional
tracer initialization and general diagnostics using equivalent PV latitude-potential-
temperature coordinates, *Q. J. R. Meteorol. Soc.*, *121*(521 PtA), 187–210, 1995.
- Lary, D. J., and H. Y. Mussa, Using an extended kalman filter learning algorithm for
feed-forward neural networks to describe tracer correlations, *Atmospheric Chemistry
and Physics Discussions*, *4*, 3653–3667, 2004.
- McHugh, M., B. Magill, K. A. Walker, C. D. Boone, P. F. Bernath, and J. M. Russell,
Comparison of atmospheric retrievals from ace and haloe, *Geophys. Res. Lett.*, *32*(15),
0094-8276 L15S10, 2005.
- Nassar, R., et al., A global inventory of stratospheric chlorine in 2004, *J. Geophys. Res.*
(*Atmos.*), *111*(D22), 0148-0227 D22312, 2006.
- Newman, P. A., E. R. Nash, S. R. Kawa, S. A. Montzka, and S. M. Schauffler, When will
the antarctic ozone hole recover?, *Geophys. Res. Lett.*, *33*(12), 2006.
- Offermann, D., K. U. Grossmann, P. Barthol, P. Knieling, M. Riese, and R. Trant, Cryo-
genic infrared spectrometers and telescopes for the atmosphere (crista) experiment and
middle atmosphere variability, *J. Geophys. Res. (Atmos.)*, *104*(D13), 16,311–16,325,

1999.

Proffitt, M., et al., Insitu ozone measurements within the 1987 antarctic ozone hole from a high-altitude ER-2 aircraft, *J. Geophys. Res. (Atmos.)*, *94*(D14), 16,547–16,555, 1989.

Roche, A. E., J. B. Kumer, J. L. Mergenthaler, G. A. Ely, W. G. Uplinger, J. F. Potter, T. C. James, and L. W. Sterritt, The cryogenic limb array etalon spectrometer (CLAES) on UARS - experiment description and performance, *J. Geophys. Res. (Atmos.)*, *98*(D6), 10,763–10,775, 1993.

Russell, J. M., et al., The Halogen Occultation Experiment, *J. Geophys. Res. (Atmos.)*, *98*(D6), 10,777–10,797, 1993.

Russell, J. M., et al., Validation of hydrogen chloride measurements made by the halogen occultation experiment from the UARS platform, *J. Geophys. Res. (Atmos.)*, *101*(D6), 10,151–10,162, 0148-0227, 1996.

Schoeberl, M. R., L. C. Sparling, C. H. Jackman, and E. L. Fleming, A lagrangian view of stratospheric trace gas distributions, *J. Geophys. Res. (Atmos.)*, *105*(D1), 1537–1552, 2000.

Schoeberl, M. R., et al., Reconstruction of the constituent distribution and trends in the antarctic polar vortex from er-2 flight observations, *J. Geophys. Res. (Atmos.)*, *94*(D14), 16,815–16,845, 1989.

Waugh, D., and T. Hall, Age of stratospheric air: theory, observations, and models, *Reviews of geophysics*, *2000RG000101*(10.1029), 2002.

WMO, Scientific assessment of ozone depletion: 2006, *Tech. Rep. 50*, WMO Global Ozone Res. and Monitor. Proj., Geneva, 2006.

213 Zander, R., M. R. Gunson, C. B. Farmer, C. P. Rinsland, F. W. Irion, and E. Mahieu, The
214 1985 chlorine and fluorine inventories in the stratosphere based on atmos observations
215 at 30-degrees north latitude, *J. Atmos. Chem.*, 15(2), 171–186, 1992.

Instrument	Temporal Coverage	Species	References	Median Observation Uncertainty
ACE	2004-2006	HCl, ClONO ₂ and ClO	<i>Bernath et al.</i> [2005]	8% (HCl), 30% (ClONO ₂), >100% (ClO)
ATMOS	1991, 1993, 1994	HCl, ClONO ₂	<i>Zander et al.</i> [1992]	8% (HCl), 60% (ClONO ₂)
Aura MLS	2004-2006	HCl and ClO	<i>Froidevaux et al.</i> [2006]	12% (HCl), 76% (ClO)
CLAES	1991-1993	ClONO ₂	<i>Roche et al.</i> [1993]	>100%
CRISTA	1994, 1997	ClONO ₂	<i>Offermann et al.</i> [1999]	61%
HALOE	1991-2005	HCl	<i>Russell et al.</i> [1993]	4%

Table 1. The instruments and constituents used in constructing the Cl_y record from 1991-2006. The uncertainties given are the median uncertainties of the level 2 product for all the observations made.

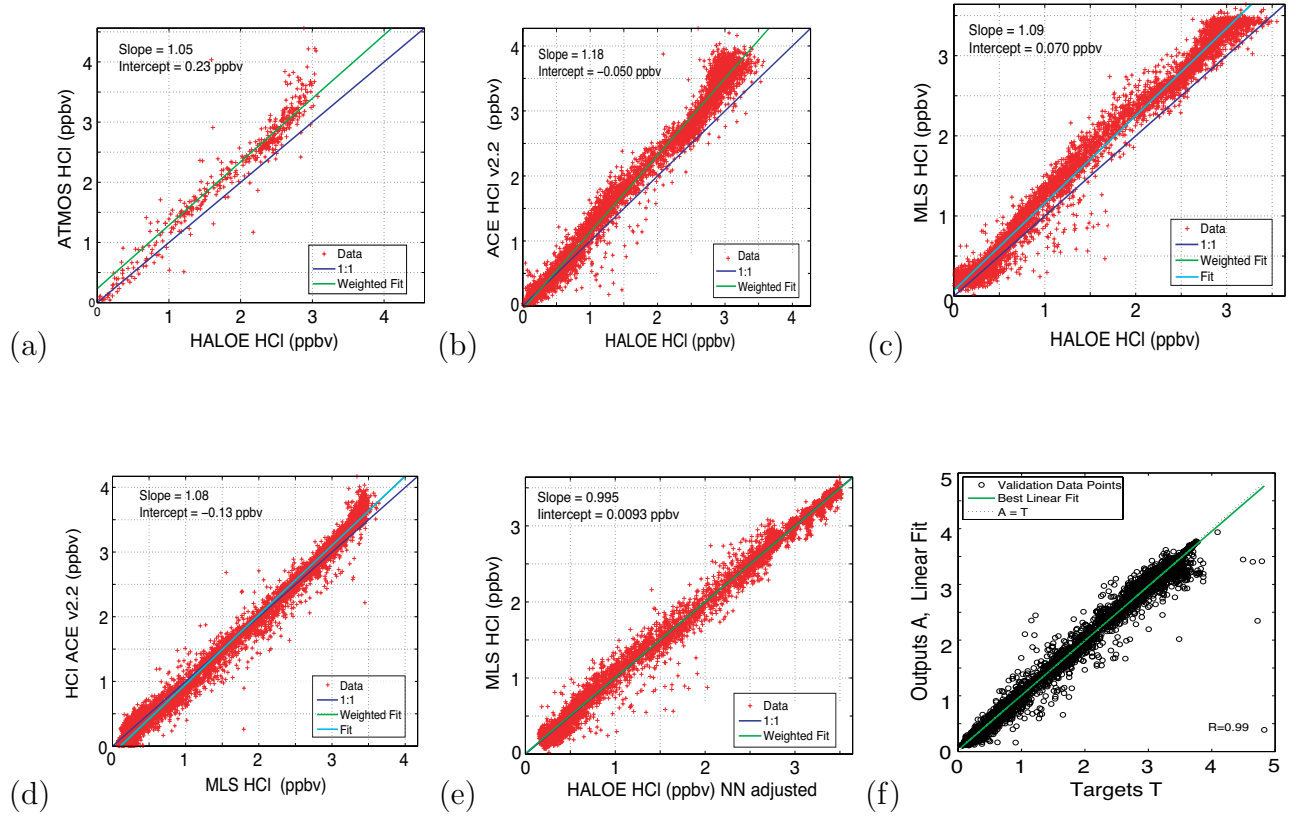


Figure 1. Panels (a) to (d) show scatter plots of all contemporaneous observations of HCl made by HALOE, ATMOS, ACE and MLS Aura. In panels (a) to (c) HALOE is shown on the x-axis. Panel (e) correspond to panel (c) except that it uses the neural network ‘adjusted’ HALOE HCl values. Panel (f) shows the validation scatter diagram of the neural network estimate of Cl_y versus the actual Cl_y for a totally independent data sample *not* used in training the neural network.

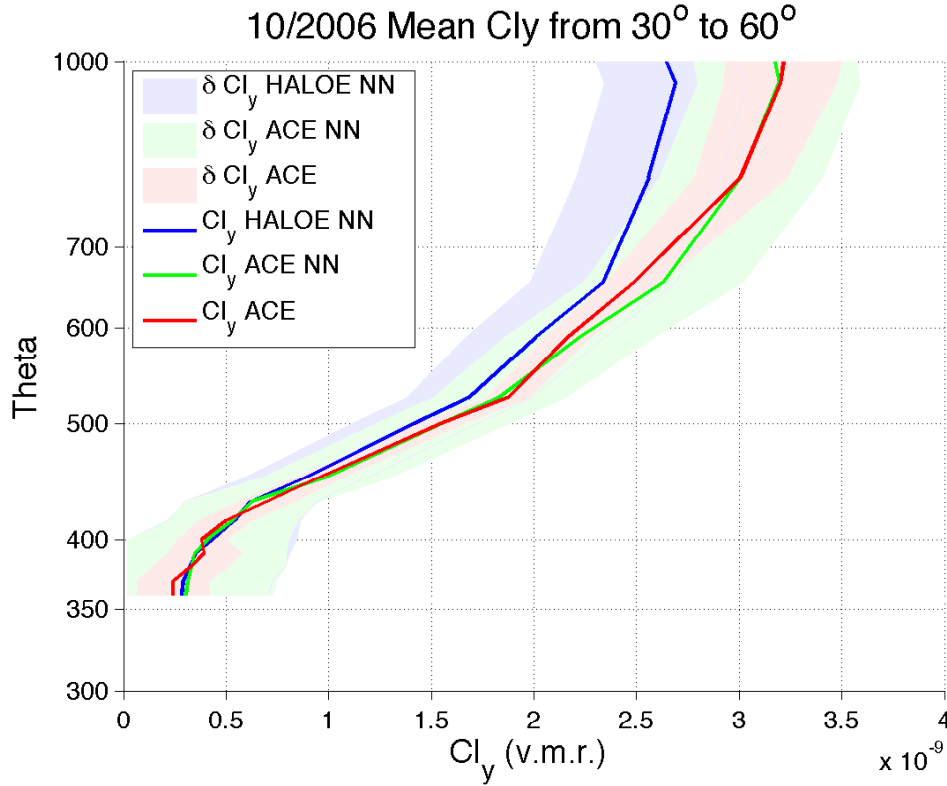


Figure 2. Cl_y average profiles between 30° and 60°N for October 2006. The blue line shows the Cl_y estimated by a neural network using HCl observations calibrated to agree with HALOE v19 HCl. The green line shows the Cl_y estimated by a neural network using HCl observations calibrated to agree with HALOE v19 HCl. The red line shows observed $\text{Cl}_y = \text{HCl} + \text{ClONO}_2 + \text{ClO}$ based on ACE v2.2 data. In each case the shaded range represents the uncertainty associated with the Cl_y estimate.

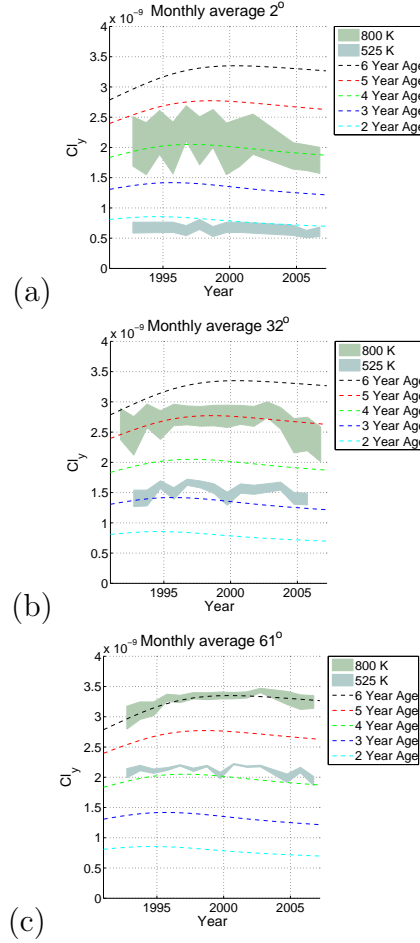


Figure 3. Panels (a) to (c) show October Cl_y time-series for the 525 K isentropic surface (≈ 20 km) and the 800 K isentropic surface (≈ 30 km). In each case a shaded range representing the uncertainty in our estimate of Cl_y is shown. This uncertainty is due to the biases between the various HCl observations. The upper limit of the shaded range corresponds to the estimate of Cl_y based on all the HCl observations calibrated by a neural network to agree with ACE v2.2 HCl. The lower limit of the shaded range corresponds to the estimate of Cl_y based on all the HCl observations calibrated to agree with HALOE v19 HCl. Overlaid are lines showing the Cl_y based on age of air calculations [Newman *et al.*, 2006]. To minimize variations due to differing data coverage Months with less than 100 observations of HCl in the equivalent latitude bin were left out of the time-series.